Structural Eng./Earthquake Eng., JSCE, Vol. 20, No. 2, 119s–130s, 2003 July
(J. Struct. Mech. Earthquake Eng., JSCE, No. 738/ I —64)

FATIGUE EVALUATION OF STEEL POST STRUCTURES

Zhi-Gang XIAO[1] and Kentaro YAMADA[2]

[1]Student Member of JSCE, M. Eng., Dept. of Civil Eng., Nagoya University
(Furocho, Chikusa-ku, Nagoya 464-8603, Japan)
[2]Member of JSCE, Ph.D., Professor, Department of Environmental Engineering and Architecture, Graduate School of Environmental Studies, Nagoya University (Furocho, Chikusa-ku, Nagoya 464-8603, Japan)

In post structures supporting traffic signs or lighting apparatuses on highway bridges, strengthening gussets welded at the bottom of post introduce stress concentration and make these details susceptible to fatigue failure. Stress and deformation near critical points in normal and improved type post structures are comprehensively studied with 3D finite element analyses. Fatigue evaluations are carried out with HSS method and one-millimeter stress approach based on finite element analyses. Fatigue strengths are suggested based on test data and evaluations. It is found that one-millimeter stress approach is suitable for fatigue evaluation of post structures and that thickness correction is necessary in HSS method evaluations.

Key Words : *fatigue, HSS (hot spot stress), traffic sign post, lighting post, gusset, 3D FEM (finite element method)*

1. INTRODUCTION

Steel posts are usually used to support lighting apparatuses and traffic signs on highway bridges in Japan, **Fig.1**. The bottom end of the post is normally welded to a baseplate, which in turn is attached to the bridge structure through several high-strength anchor bolts. To strengthen the connection between the post and the baseplate, four or eight triangular gussets are usually welded to both the post and the baseplate. The gussets increase section modulus of the post, but introduce stress concentration at gusset tips. Vibration of the post caused by the passing traffics and/or wind loading may generate essential cyclic stresses at gusset tips and initiate fatigue cracks there.

Fatigue was not taken into consideration in the design of highway bridges in Japan until March 2002 when the guidelines for fatigue design[1)] was published. Cases of fatigue failure of steel post structures have been reported both in Japan[2)] and overseas[3),4)], and the problem of fatigue of post structures has been brought into concern in recent years. The remaining fatigue life of existing post structures should be evaluated in an exact way for the purpose of proper maintenance, and new types of post structures with high performance of fatigue-resistance should be suggested for future design to avoid fatigue failure.

In this study, stress concentration and deformation at critical points are comprehensively studied with 3D FEM analyses for the normal type and two improved types of post structures, and fatigue estimations are carried out with both hot spot stress (HSS) method and one-millimeter stress approach. Available fatigue test results are also presented, and fatigue strengths are suggested based on test data and evaluations. It is found that one-millimeter stress approach is suitable for evaluating fatigue lives of post structures and that thickness correction is necessary in HSS evaluations.

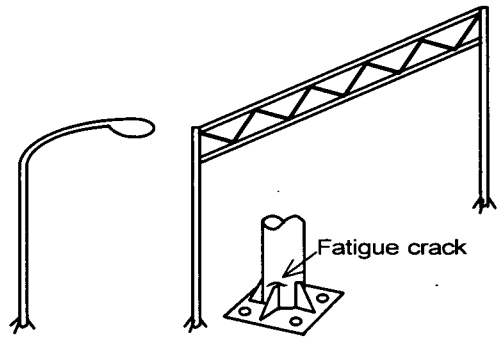

Fig.1 Fatigue crack in normal type post structures.

2. FATIGUE EVALUATION APPROACHES

(1) Classification method

If focusing on the stress concentration at gusset tip, the detail of out-of-plane gusset may be the most similar to post-baseplate connection. In the fatigue design recommendations of Japanese Society of Steel Construction (JSSC), the out-of-plane gusset is classified into Category F (65MPa at 2 million cycles), when the weld is as-welded and the length of the gusset is less than or equal to 100mm, or Category G (50MPa at 2 million cycles) when the weld is as-welded and the gusset is longer than 100mm[5]. Since the triangular gussets in the post-baseplate connection are usually longer than 100mm, the fatigue life of the connection might be approximated with JSSC-G Category.

(2) HSS method

Most of the fatigue design guidelines or recommendations[5)-8)] recommend HSS method as a fatigue evaluation approach. The International Institute of Welding (IIW) gives detailed suggestions on the application of HSS[9)]. When the membrane stress is dominant in the vicinity of critical points, IIW suggests linear extrapolation to get the HSS at weld toe, **Fig.2**, with the first extrapolation point being $0.4t$ (t, thickness of main plate) away from the weld toe and the second extrapolation point being $1.0t$ away from toe. In the case of shell bending stresses, IIW suggests quadratic extrapolation. For as-welded fillet welded details, the fatigue resistance against HSS is suggested as FAT 100 (100MPa at 2 million cycles), with the slope of S-N curve being taken as 1/3.

(3) One-millimeter stress approach

Focusing on the stress distribution along the expected path of fatigue crack, the writers suggest an approach to evaluating fatigue life of fillet welded structural details[10)]. It is found by FEM analyses that, along the direction of crack propagation, the local effect of weld profile is limited within 1mm from crack origin (weld toe), **Fig.3**. The stress at this location (1mm in depth, in most cases) is rationally taken as an indicator of geometric effect, i.e. effect of the geometries of other elements except weld profile, and is used as a quantity for evaluating fatigue strength of fillet welded details.

The S-N curve to be used with stresses at one millimeter in depth is determined with test data of non-load-carrying fillet welded cruciform joints, **Fig.4**. In these cruciform joints (hereinafter referred to as reference details), weld profile is the dominant contributing factor to stress concentration at weld toe region, and the scatter of test data reflects primarily the variation of weld profile. The thickness of main plate and attachments in the reference detail is 10mm, and the leg length of the equal leg fillet welds is about 6mm. FEM analysis demonstrates that stress concentration factor at 1mm in depth in these joints is close to unity. Fatigue test results of non-load-carrying cruciform joints show that wider specimens tend to have lower fatigue strength. Width of reference details is limited to a small range to exclude width effect.

The applicability of this one-millimeter stress approach to fillet welded joints is verified by fatigue test results of several typical details, such as in-plane gussets and out-of-plane gussets[10)].

3. FEM ANALYSES OF NORMAL TYPE OF POST STRUCTURE

(1) FEM model

A 3D model of eight-node solid element is created for the normal type of post structure shown in **Fig.5(a)**, using the software package COSMOS/M

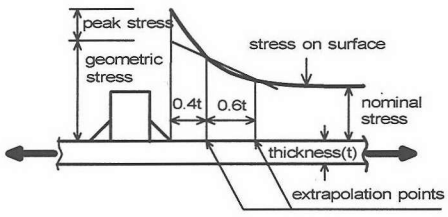

Fig.2 Hot spot stress method.

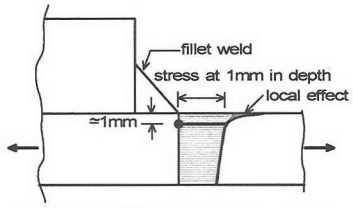

Fig.3 One-millimeter stress approach.

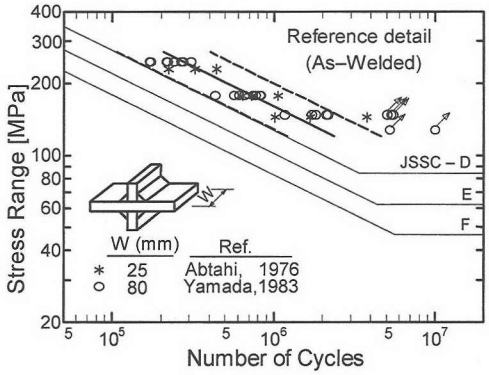

Fig.4 Fatigue test data of reference detail.

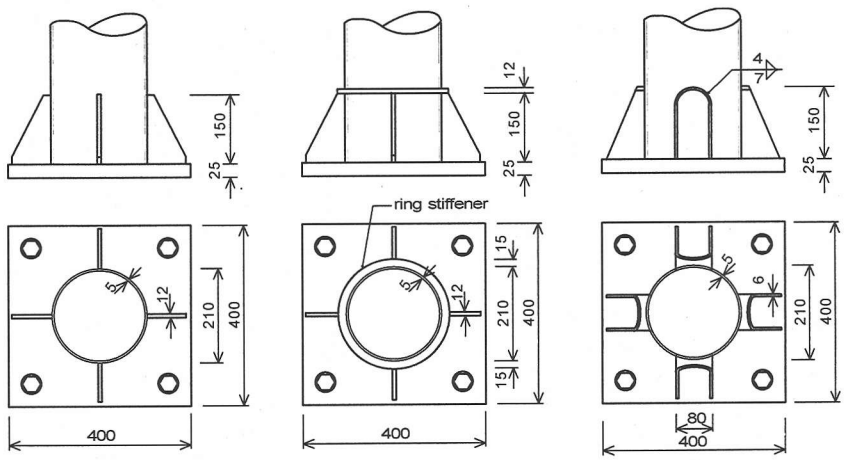

(a) normal type **(b)** ring-strengthened type **(c)** U-stiffener type

Fig.5 Partial elevations and plan views of post structures (unit in millimeter).

2.6[11]. By taking advantage of symmetry, only one quarter of the structure is modeled, **Fig.6**. The length of the pipe segment is taken as 560mm. It is about twice the post diameter from gusset tip to the top surface of the pipe segment. Tensile loading corresponding to the nominal stress of 1MPa is applied on the top surface of the post segment. As will be shown subsequently, the simple tensile loading case can result in comparable stress concentration at the critical point, gusset tip, as the bending case. The bolts are located at four corners of the baseplate, and the distance from the center of the bolt to the side of the baseplate is 50mm. Vertical translation of nodes on the bottom surface of baseplate within affecting region of bolt is constrained. The affecting region of bolt is taken as a circular area whose diameter equals to bolt diameter (25mm) plus twice thickness of the baseplate.

Gusset tip region. Fillet weld of 6mm leg length is modeled with zero-radius weld toes. The corner of turnaround weld at gusset tip is modeled with a quarter of a cone, and special efforts are made in meshing the part of post adjacent to this corner so that the elements in the vicinity of corner have comparable size to those in front of the gusset tip. The main reason for doing this is that the stress gradient in the vicinity of turnaround weld at gusset tip is rather high, and mesh size will have significant influence on the value of calculated stress. The mesh size at this region is set at 1x1x1mm. Away from the weld toe, five rows of 1mm, and next five rows of 2mm long elements are meshed.

Post-baseplate weld. The fillet weld joining the bottom end of the post to the baseplate (hereinafter referred to as post-baseplate weld) is also modeled with fine mesh.

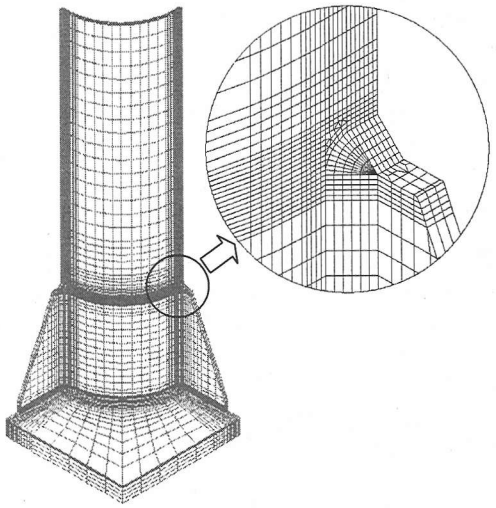

Fig.6 A quarter model of the normal type post structures.

Gusset-baseplate weld. The fillet weld connecting the gusset to the baseplate is neglected because of the difficulties encountered in modeling three perpendicularly intersecting welds at the corner where the gusset meets both the post and the baseplate. The absence of the gusset-baseplate weld does not have significant effect on the stress concentration at gusset tip, which is about 150mm away from this weld. Besides, the stress concentration along this weld is not so severe as that along the post-baseplate weld, and there is less possibility of fatigue cracking along this weld. FEM analyses also show that the severity of stress concentration at the intersecting corner is far less than that at the middle part of the post-baseplate weld in between neighboring gussets. In engineering practice, a cope

hole is often cut at gusset corner to avoid intersection of multiple welds. This treatment may have some effects on stress at critical points and should be reflected by FEM models.

The unwelded zone between gusset and post wall is modeled by disconnecting neighboring elements at both sides of the contacting interface. This is done by setting coinciding nodes on the interface. One of the coinciding nodes belongs to post wall element, the other to gusset element. The wall of the post is modeled with five layers of elements, each 1mm thick. Total number of elements and nodes of the quarter model is 39,980 and 46,485, respectively. The Young's Modulus is taken as 207GPa, and Poisson Ratio as 0.3.

(2) Stress distribution under axial loading

FEM analysis shows that there is a severe stress concentration near the toe of turnaround weld at gusset tip. Stress distribution along three directions at this region is shown in **Fig.7** with solid lines. The origin of the coordinates is set at the midpoint of weld toe line of the turnaround welding, Point B in the inset of **Fig.7**. The results summarized in **Fig.7** are the values of the normal stress component in y-direction. Symbols such as filled circles indicate locations of nodes. Stresses at nodes shared by adjacent elements are averaged by the software. Since the nominal stress is unity, the stresses in **Fig.7** actually represent stress concentration factors.

x-axis distribution. **Fig.7(a)** is the stress distribution through the thickness of post wall. It is seen that the outside surface (x=0) is in tension while the inside surface (x=5mm) is in compression. The compression stress state of the inside surface indicates that significant local bending occurs at gusset tip.

y-axis distribution. **Fig.7(b)** shows surface stress distribution in the direction parallel to post axis. Beyond the node at 3mm away from weld toe, stress gradient becomes less steep, but it takes more than 60 mm for the stress to descend to the level of nominal stress. This indicates that the peak stress caused by the weld profile is limited within a rather small region while the affecting region of gusset is relatively large.

The other phenomenon shown in **Fig.7(b)** is that the stress value at the first node (y=0) is less than that at the second node (y=1mm). The reason behind this is that the stress at a node presented here is actually the averaged value among elements sharing this common node. Since the nodal stresses of elements within the weld profile are relatively small, the averaged stress at the first node goes down. This is opposite to the singular feature at a sharp notch tip[12]. Since the stress value at weld toe is not of special interest in this study, the cross-weld averaging is just followed.

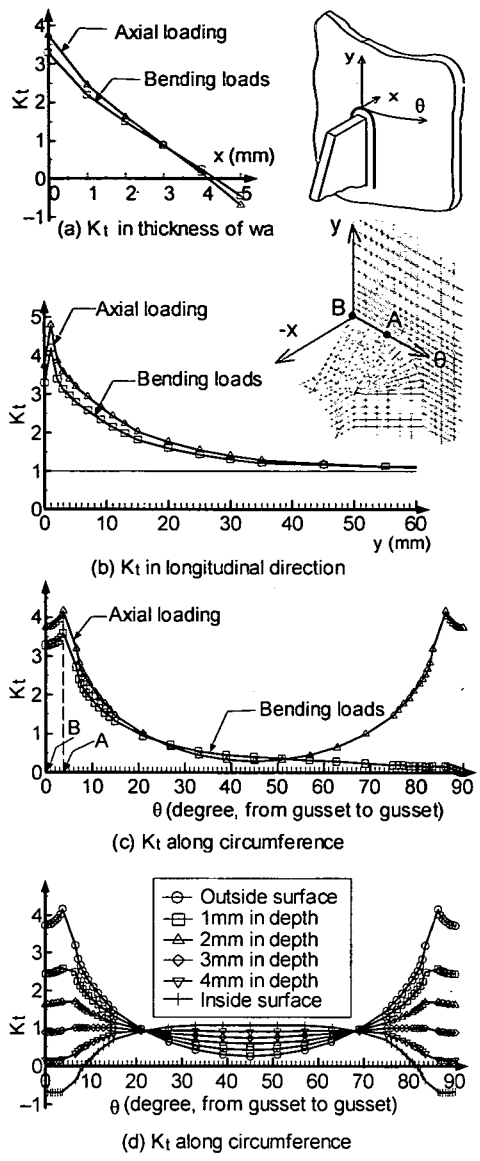

Fig.7 Stress distribution of normal type.

θ-axis distribution. To have a complete understanding on the stress concentration at gusset tip region, stress distribution on the cross section passing through turnaround weld toe is presented in **Figs.7(c)** and **(d)**. The abscissas indicate the location of a node, expressed in terms of the angle between the vertical plane passing the node and the post axis and the mid-thickness central plane of the reference gusset. **Fig.7(c)** shows stress distribution on the outside surface, while **Fig.7(d)** presents results through post wall thickness, giving a whole

picture of stress distribution on the cross section at gusset tip level.

On the outside surface, there exists high stress concentration near gusset tip, and stress falls below unity (nominal stress) at the middle part in between neighboring gussets. It should be noted that, along weld toe, stress does not get maximum value at the midpoint of turnaround weld, Point B in the inset of **Fig.7**, but at the intersection of the straight weld toe and the curved weld toe, Point A. The abrupt stress change from Point B to Point A seems difficult to understand since there is no abrupt change of geometry within this small region. It may result from the specific geometry of turnaround weld model or the averaging of nodal stress across weld. Further inward along other cylindrical surfaces, this kind of stress change becomes less steep, **Fig.7(d)**, and the $K_{t,global}$ that will be used later to evaluate fatigue life is still taken at the central plane of gusset in accordance with past practice.

(3) Deformation under axial loading

To give a full picture of the behavior of the post structure, the deformation under axial loading is presented in **Figs.8** and **9**. **Fig.8** shows schematically the deformed shape. The largest deformation occurs at the level of gusset tip. At this level, the part of post wall in between gussets deforms inward while the part close to gusset tip deforms outward. The "warp" of the baseplate caused by the constraint of anchor bolt can also be seen. **Fig.9(a)** shows the radial displacements of nodes on outside surface of post at the level of turnaround weld toe, i.e. the level of AB weld toe line in the inset of **Fig.7**. Positive values indicate outward deformations and negative ones inward deformations. The maximum outward displacement of 0.0018mm occurs at Point B (see the inset in **Fig.7** for its location) while the maximum inward displacements of 0.0013mm at the midpoint node in between neighboring gussets (θ= 45deg). To give a visualized description, the deformed shape of outside surface at Point B level is plotted in **Fig.9(b)** with deformation values magnified 10,000 times. The deformed shape of the post wall in vertical direction is shown by picking up the maximum outward and inward deformation outlines, **Fig.9(c)**. It is seen that beyond 400 mm above the baseplate, these two outlines tend to coincide. This means that the warp of the post wall fades out at about 400mm above the baseplate (about 250mm

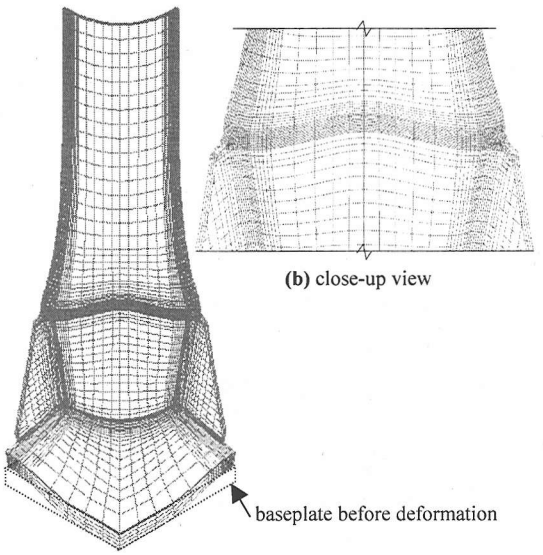

(b) close-up view

(a) the whole view of the model

Fig.8 Magnified deformation.

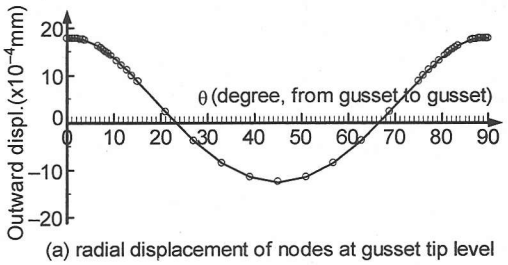

(a) radial displacement of nodes at gusset tip level

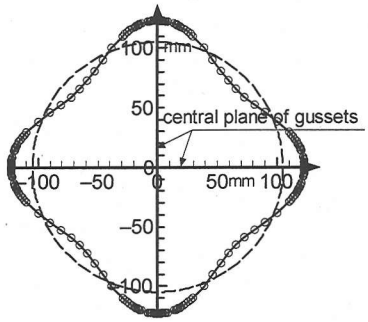

(b) Deformed section at gusset tip level
(deformation magnified 10,000 times)

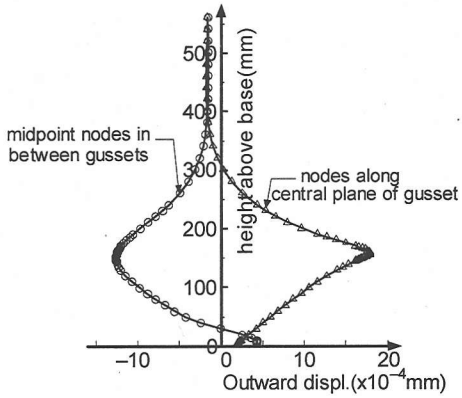

(c) deformation outline (longitudinal direction)

Fig.9 Deformations under axial loading corresponding to nominal stress of 1MPa.

above the gusset tip), and the nominal shrinkage deformation of the post wall under tension shows.

(4) Shell element model

The construction of the abovementioned 3D solid element model is time-consuming, but may give a more detailed and faithful description of the structural behavior than the shell element model. The post structure of normal type in **Fig.5(a)** is also modeled with shell elements for the purpose of comparison. The post, gusset, and baseplate are modeled in their mid-thickness planes with the COSMOS/M SHELL4 element. The presence of fillet weld is neglected in the model. SHELL4 is a 4-node quadrilateral thin shell element with membrane and bending capabilities for the analysis of three-dimensional structural models. The shear deformation effect is neglected[11].

Stress distributions around gusset tip along y- and θ-directions are presented in **Fig.10**. Stress variation through the thickness of post wall (x-direction) cannot be obtained from shell element models. For comparison, the previous stress results on outside surface of solid element model are also plotted in **Fig.10** with solid lines and triangle symbols. It is shown that shell model results in much higher stress concentration at gusset tip. Stress gradient becomes steeper in both y- and θ-directions in the vicinity of gusset tip. If the shell element results are compared with the solid element stresses at the mid-thickness surface of post wall, **Fig.10**, even larger differences will be shown. The discrepancy between these two models is mainly caused by the modeling of weld profile. The neglect of weld geometry in the shell model makes the notch effect at gusset tip much more severe.

(5) Stress distribution under bending loads

Pure bending loads are applied on the top surface of the post segment. In post structures, the flexural stresses at the post-baseplate connection region are usually caused by a lumped mass, e.g., signboard, which is usually at the level of several meters above baseplate. Shear stresses at the post-baseplate connection region are negligibly small compared with the flexural stresses, and the loading case of pure bending is suitable for demonstrating the post structure behaviors.

The previous quarter model under axial loading is reused, with the symmetric boundary conditions on one of the symmetric planes replaced by anti-symmetric ones.

Stress distribution near the tip of tensile gusset is also plotted in **Fig.7** for bending loads. The stress distribution pattern is similar to that under axial loading in x- and y-directions. In θ-direction (circumferential direction), along the half-length close to the tensile gusset (θ=0~45deg), stress distribution is similar to axial loading, while along the other half-length the stress further decreases, until down to zero at the gusset along the neutral axis (θ=90deg).

Stress concentration at the turnaround weld of tensile gusset is slightly reduced compared with the axial loading case, but the difference is not substantial.

4. FACTORS AFFECTING STRESS CONCENTRATION AT CRITICAL POINTS

(1) Geometric parameters

Four geometric parameters, i.e. thickness of post wall t_w, thickness of baseplate t_b, post diameter D, and gusset length L, **Fig.11**, are thought to have effects on stress concentration at gusset tip. Their effects are studied with four FEM models under axial loading. These models, Model A, B, C, and D, have the same dimensions as the basic model in **Fig.5(a)** except that shown in bold font in **Table 1**. The stress concentration factor at 1mm in depth at critical point, $K_{t,global}$, of each model, and their relative values to the basic model are listed in **Table 1**. If assuming monotonic change of $K_{t,global}$ with each parameter, the following conclusions can be drawn. Stress concen-

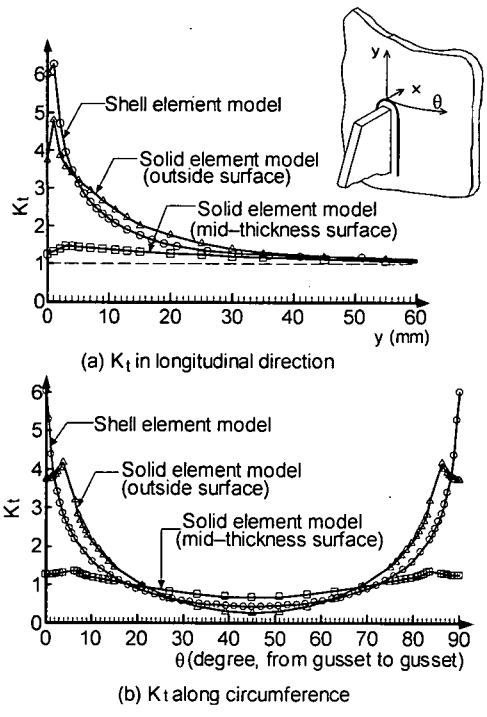

Fig.10 K_t of shell element and solid element models.

tration at gusset tip increases with the increase in post wall thickness, and decreases with the increase in baseplate thickness, post diameter, or gusset length.

As thickness of post wall increases, stress gradient in the thickness direction at gusset tip becomes less steep, and therefore the stress concentration at 1mm in depth becomes relatively large. A thick baseplate has large out-of-plane stiffness, and therefore can reduce outward deformation at gusset tip and result in decreased stress concentration.

The increase of gusset length leads to slight decrease in stress concentration at gusset tip, this is opposite to the normal case of non-load-carrying out-of-plane gusset[10]. This may be related with the load transmitting function of the gusset.

Increase of post diameter helps to reduce the misalignment between anchor bolt and post wall, thus lessens the outward deformation and stress concentration at gusset tip. It seems that the location of bolt plays an important role. To prove this, a new model, Model C' is created by shifting the bolt in Model C towards the center of post, to the point of 115mm away from post center. The $K_{t,global}$ of Model C' is only 1.97, 74 percent of Model C. This shows that the location of bolts indeed plays a crucial role in affecting $K_{t,global}$.

(2) Boundary conditions of baseplate

As an extreme case, all the nodes on the bottom surface of the baseplate in the basic model are vertically constrained, and a $K_{t,global}$ of 1.98 is resulted, being comparable to that of Model C'. The addition of vertical constraint on the whole bottom surface overwhelms the use of thick baseplate in reducing outward deformation at gusset tip and hence decreases stress concentration significantly.

(3) Post-baseplate connection

The other type of post-baseplate connection, socket connection, is often found in post structures. In a socket connection, the post is inserted into a hole cut in the center of the baseplate, **Fig.11(d)**. With modification on the basic model, a socket connection model is created and analyzed. An increased $K_{t,global}$ of 2.75 is obtained due to stiffness loss of baseplate caused by cutting the hole.

(4) Discussions

As shown above, increasing the out-of-plane stiffness of the baseplate by using thick baseplate can reduce stress concentration at gusset tip. By contrast, adding vertical constraint to the bottom surface of the baseplate or moving the anchor bolts close to post center are more effective in reducing stress concentration. However, it is much difficult to

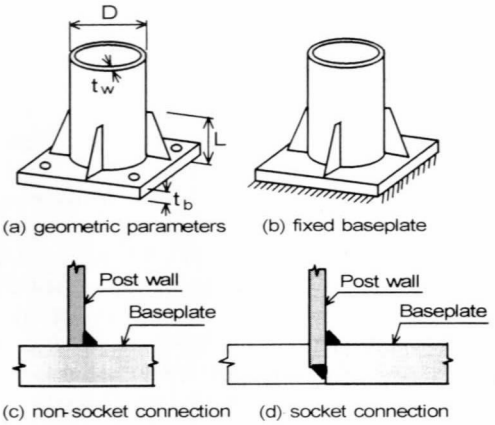

Fig.11 Factors affecting stress concentration.

Table 1 Basic features of FEM models and $K_{t,global}$.

Model	t_w (mm)	t_b (mm)	D (mm)	L (mm)	$K_{t,global}$	$K_{t,global}$ ratio
Basic	5	25	210	150	2.45	1
A	**8**	25	210	150	2.65	1.08
B	5	**14**	210	150	2.66	1.09
C	5	25	**114**	150	2.66	1.09
C'	5	25	**114**	150	1.97	0.804
D	5	25	210	**200**	2.39	0.976
Fixed Base.	5	25	210	150	1.98	0.808
Socket	5	25	210	150	2.75	1.12

realize the ideal boundary condition of fixed baseplate. Shifting bolts towards post center is usually prohibited since it will reduce the capability of resisting horizontal loads and increase lateral displacement of post structure. It is necessary to suggest other types of post structures to get an essential reduction in stress concentration at critical points.

5. FEM ANALYSES OF RING-STRENGTHENED AND U-STIFFENER TYPES

(1) 3D FEM models

In order to lessen the stress concentration at gusset tip, which will lead to low fatigue resistance of the post structures, two other alternatives, i.e. the ring-strengthened and U-stiffener types, are suggested, **Figs.5(b)** and **(c)**, and analyzed with 3D solid element models. The ring-strengthened type has a ring-shaped plate connecting the gusset tips to the post, and in the U-stiffener type, triangular gussets are replaced by inverted U-shaped stiffeners. As shown earlier, the axial loading can describe the stress concentration at critical points to a compara-

ble extent to the bending load. The simple axial loading case is employed again to analyze these two alternatives.

A quarter model is created for both ring-strengthened type and U-stiffener type, **Figs.12(a)** and **(b)**. The ring-post weld is of 6mm leg length and zero-radius weld toe. Weld toe regions near gusset tip are the focus of meshing. Elements of 1x1x1mm are generated within this region. The fillet welds joining the inverted U-shaped stiffener to the post are of two sizes, the outer one being 7mm in leg length and the inner one 4 mm. Weld toe radii of these welds are also set to zero. Weld toe region of the curved part of the stiffener is modeled with fine mesh of the size about 1x1x1mm. The other modeling details of these two models are similar to those of the normal type.

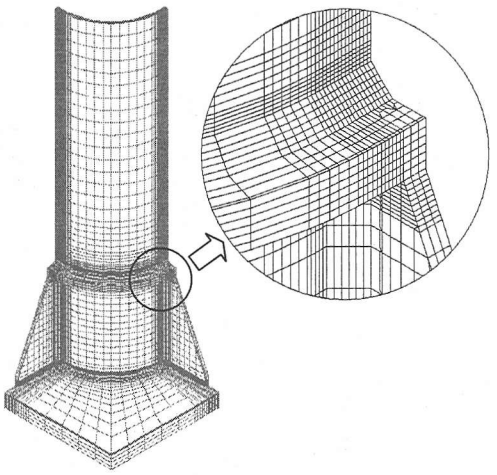

(a) A quarter model of ring-strengthened type

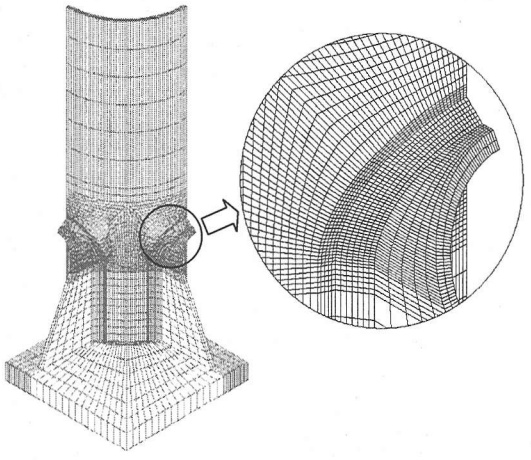

(b) A quarter model of U-stiffener type

Fig.12 FEM models of ring-strengthened and U-stiffener type.

(2) Stress concentration and deformation

Stress distributions of these two models are shown along with normal type model in **Fig.13**. In the ring-strengthened type, the origin of the coordinates is set at the point where the top weld toe outline of the ring intersects the mid-thickness central plane of the gusset. In the U-stiffener type, the origin of coordinates is set at the climax of weld toe outline of the outer welding of U-stiffener. The points where the origin of coordinates is set are the positions of critical points in these two models.

It can be seen in **Fig.13** that the stress concentration at critical points is significantly reduced, with the ring-strengthened type being slightly higher than U-stiffener type. Unlike the normal type, the inside surface of the post near the critical point is still in tension, **Fig.13(a)**. This indicates that local bending at critical point is significantly reduced. In **Fig.14**, where the radial displacement of the cross section at critical point level is shown, it can be seen that the deformation of these two types is also essentially reduced.

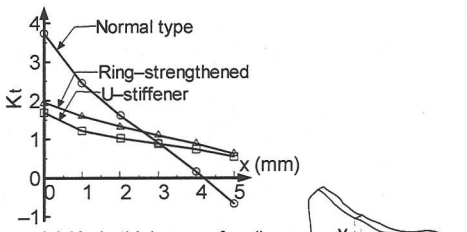

(a) K_t in thickness of wall

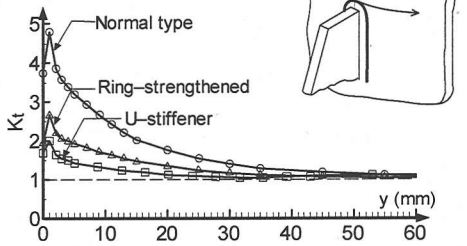

(b) K_t in longitudinal direction

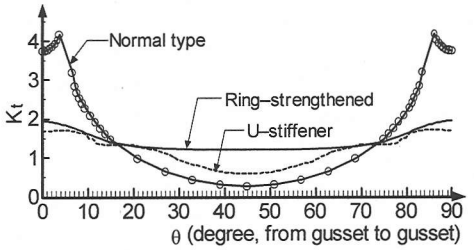

(c) K_t along circumference

Fig.13 Stress distribution of ring-strengthened and U-stiffener type.

6. FATIGUE LIFE EVALUATION AND FATIGUE TEST RESULTS

(1) Fatigue life evaluation

As an example, the steps of fatigue life estimation with HSS method and one-millimeter stress approach for the normal type post structure in **Fig.5(a)** under axial loading are described below.

a) HSS method

Extrapolation. According to IIW suggestions[9], HSS at weld toe can be obtained by linear extrapolation through the points at $0.4t$ (t, post wall thickness, 5mm) and $1.0t$ from weld toe. IIW suggests principal stresses be used for extrapolation.

Stresses. Some researchers, e.g., van Vingerde, suggest that stresses perpendicular to the weld should be used for extrapolation[13]. One of the main reasons for this is that the difference between principal stresses and stresses perpendicular to weld toe decreases closer to the weld because of the stiffening influence of the weld and attachment. The other is that only stress components perpendicular to the weld are enlarged by stress concentrations caused by the global weld shape and the attachment. The practice of extrapolating with stresses perpendicular to weld is followed here. In the case of normal type post structure, the stress component perpendicular to the weld can be further decomposed into two stress components perpendicular to each other, one along x-axis (post wall thickness direction), the other along y-axis (longitudinal direction). Since the x-axis component is negligibly small at weld toe region compared with the y-axis component, the extrapolation is further simplified by using the y-axis component so that the stress distribution results hitherto summarized can be used directly to extrapolate HSS.

Fatigue life. The y-axis stress distributions in solid model and shell model are re-plotted in **Fig.15**, focusing on the stress distribution close to weld toe. HSS factors of 4.32 and 5.78 are obtained for solid element model and shell element model, respectively, with $0.4t$ and $1.0t$ extrapolation. HSS of shell model is the result extrapolated to gusset end, since the stress at weld toe position might be non-conservative[14]. The fatigue resistance against HSS suggested by IIW for as-welded details is FAT 100 (100MPa at 2 million cycles). Thus the fatigue strength of the post structure shown in **Fig.5(a)** under axial loading can be estimated as 23MPa (100MPa/4.32) at 2 million cycles in terms of solid element analysis, or 17MPa (100MPa/5.78) at 2 million cycles in terms of shell element analysis, **Fig.16**. Both strengths are far below JSSC-H.

b) One-millimeter stress approach

In one-millimeter stress approach, the stress

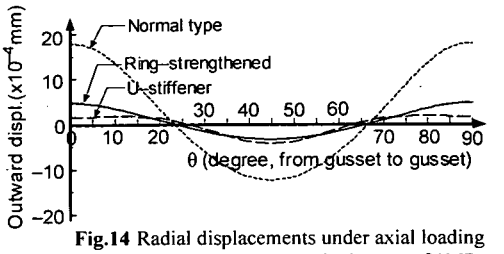

Fig.14 Radial displacements under axial loading corresponding to nominal stress of 1MPa.

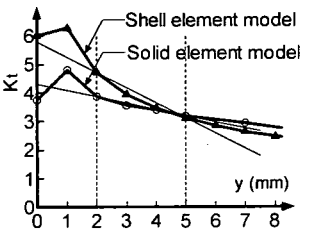

Fig.15 Solving HSS by extrapolation.

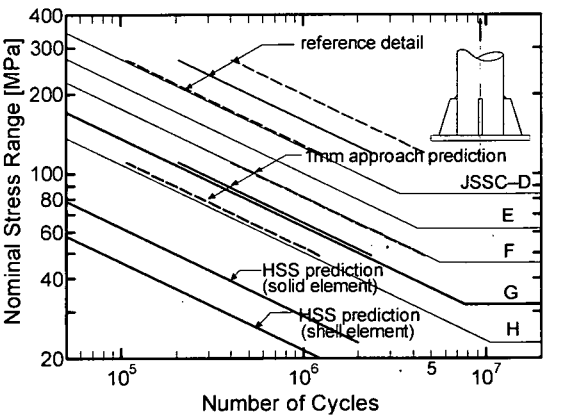

Fig.16 Fatigue life evaluation with three approaches.

concentration at 1mm in depth at critical point, termed $K_{t,global}$, is used to evaluate fatigue life of fillet welded joints. The value $K_{t,global}$=2.45 is obtained from 3D finite element analysis. The mean, mean-2s (s, standard deviation), and mean+2s of the reference data are 127MPa, 101MPa, and 158MPa at 2 million cycles, respectively. Thus the estimated mean, mean-2s, and mean+2s of this detail are 52MPa, 41MPa, and 64MPa at 2 million cycles, respectively, **Fig.16**. Following the practice of giving design fatigue strength based on mean-2s, the fatigue strength of this detail will be evaluated as 41MPa at 2 million cycles.

It is shown that there exist significant differences among these estimations. The one-millimeter stress approach results in 41MPa at 2 million cycles. HSS method leads to 23MPa (3D element) and 17MPa (shell element) at 2 million cycles.

(2) Fatigue test results and fatigue life estimation

a) Fatigue tests of small size specimen

Test results. Yamada et al.[15] carried out fatigue tests on two groups of small size post structures with tensile cyclic loadings, one group with 22mm thick baseplates, the other with thin ones (12mm). The outside diameter of the steel post of these specimens is 114mm, and the thickness of post wall is 4.5mm. The length of the four triangular gussets in each specimen is 100mm, and the center-to-center distance of the four anchor bolts is 163mm. Test results for the thick and thin baseplate groups are summarized in **Figs.17** and **18**, respectively. Thick baseplate specimens show longer fatigue life than thin baseplate ones. Test data of thick baseplate specimens are all above JSSC-G, while fatigue strength of thin baseplate ones satisfies JSSC-H.

Fatigue life estimation. Estimations in terms of stress at 1mm in depth and HSS are also presented in **Figs.17** and **18**. One-millimeter stress approach gives estimations in good agreement with the test data of thick baseplate specimens. All test data fall within the range of estimation except the two run-outs marked with arrows. A run-out is the fatigue test result of a specimen that has not shown fatigue cracks after a certain large number of cycles of loading. In the case of thin baseplate specimens, the two test data in high stress range fall just out of the range of estimation, but reasonable agreement between the data and estimation is still reached.

HSS method gives excessive underestimations for both groups. HSS estimations in terms of shell element stresses are not presented, but it can be expected that even lower fatigue strength would be obtained if shell element stresses were used, since shell element analysis results in higher stress concentration and steeper stress gradient near gusset tip, as shown previously.

The underestimation of HSS may be due to the neglect of thickness effect. In the fatigue design recommendations of IIW, thickness effect on fatigue strength is only considered for plates thicker than 25mm[9]. The strength reduction factor is calculated as follows.

$$f(t) = (25/t)^n \qquad (1)$$

where the thickness of main plate, t, should be greater than 25mm. The thickness correction component n for tubular joints is taken as 0.4. The gusset-post connection in post structures is different from the tubular joint, which usually refers to pipe-to-pipe connection in offshore structures. The value of thickness correction component n=0.3 suggested by Niemi and Marquis[14] for bracket end joint maybe more suitable for gusset-post connection. In

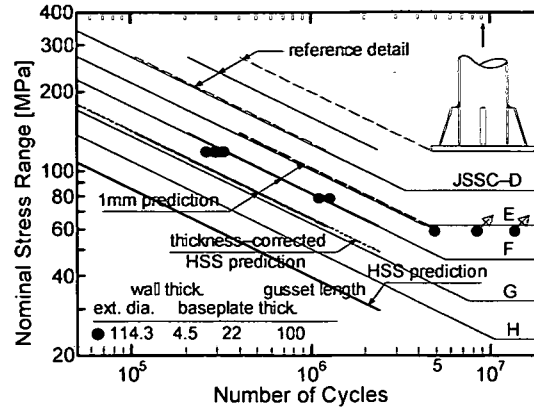

Fig.17 Fatigue life evaluation and test data.

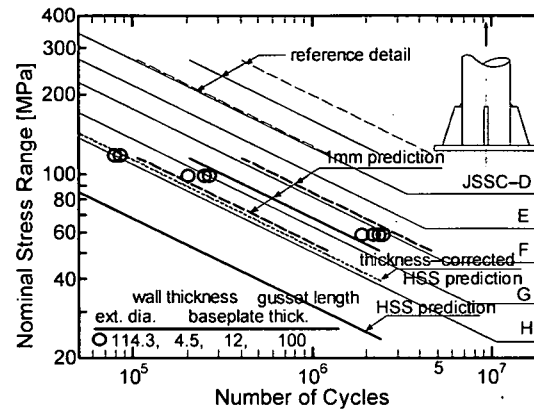

Fig.18 Fatigue life evaluation and test data.

these two groups of specimens, the thickness of the post wall is far smaller than the reference, 25mm. If strength-increasing effect due to small thickness is taken into account with the same formula as in Eq.1 and n taken as 0.3, the fatigue strength may be increased $(25/4.5)^{0.3}$ = 1.67times. The HSS estimations of solid model with thickness correction are plotted with thin dotted lines in **Figs.17** and **18**. These estimations are in good agreement with test data and predictions of one-millimeter stress approach. Since the shell element model results in much discrepancy from the solid model, even with thickness correction, the HSS evaluations based on shell element analysis are far away from test data and estimation of one-millimeter stress approach.

Unlike the extrapolation points of HSS method, the characterized point of one-millimeter in depth can pick up thickness effect, and therefore thickness effect consideration is not necessary in one-millimeter stress approach.

b) Fatigue tests of Nippon Steel Corporation

Test results. Nippon Steel Corporation[16] carried out fatigue tests on post structures of normal type and U-stiffener type. The outside diameter of the

post is 180mm, and the thickness of the post wall is of two kinds, 4.5mm and 6mm. Other dimensions are the same as those listed in **Figs.5(a)** and **(c)**. Alternating transverse load is applied on the top end of the pipe segment at the level of 1m above baseplate. Test results are presented in **Figs.19** and **20** for normal type and U-stiffener type specimens, respectively. All test data of normal type are above JSSC-G except one in high stress range, which is just below JSSC-G. All the specimens of U-stiffener type show high fatigue strength, around or above JSSC-B Category, **Fig.20**, which is comparable to the fatigue strength of parent metal. The high fatigue strength of U-stiffener may be due to the favorable profile of weld bead or the possible existence of high compressive residual stresses, which might be induced by the complex 3D geometry of the U-stiffener. Of the seven test data, two are run-outs. There are also two specimens cracked at the stiffener-baseplate welds. They are also marked as run-outs with an arrow in the figure as no cracks are found along the stiffener-post welds. The presence of fatigue cracks at both stiffener-post and stiffener-baseplate connections indicates that the stress concentration of stiffener-post connection is substantially decreased, being comparable to that of stiffener-baseplate connection.

Fatigue evaluation for normal type. One-millimeter stress approach shows some difference between the evaluations for 4.5 and 6 mm thick post walls, **Fig.19**, though the influence of post wall thickness cannot be seen evidently from the test results. Six data are available, four for 4.5mm and two for 6mm wall. Probably due to factors such as favorable weld profile, two specimens show extremely higher strength (between JSSC-E and D), which increases the scatter of data. Except these two data, well agreement is reached between evaluation of one-millimeter stress approach and test data. HSS of 6mm wall is smaller, thus fatigue strength is higher than 4.5mm wall. With thickness correction, HSS method gives almost the same fatigue strength for 4.5 and 6mm walls. As in the case of small size specimens, thickness corrected HSS estimations are in well agreement with the lower bounds of the estimations of one-millimeter stress approach, and HSS without thickness corrections leads to excessive underestimations.

Fatigue evaluation for U-stiffener type. The one-millimeter SCF of 4.5mm wall is close to one, thus U-stiffener posts of 4.5mm wall have almost the same fatigue strength as the reference details, while the evaluation of one-millimeter stress approach for 6mm wall U-stiffener is slightly lower, **Fig.20**. However, the evaluations for both are evidently lower than test results, due probably to the

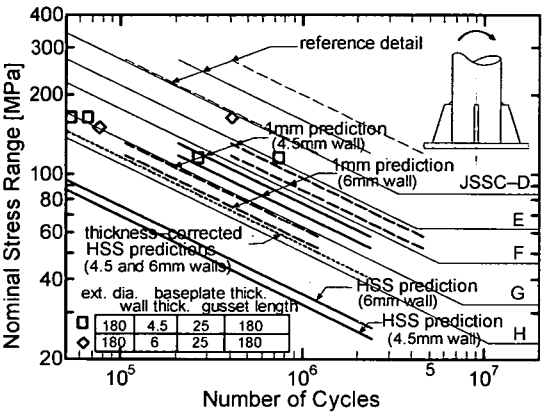

Fig.19 Fatigue life evaluation and test data.

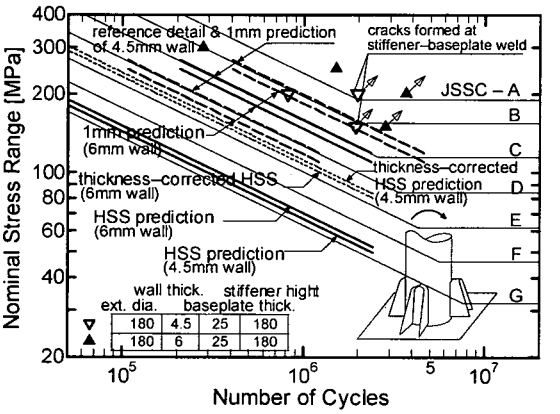

Fig.20 Fatigue life evaluation and test data.

strength-increasing factors mentioned above. As in the case of normal type, HSS results in higher estimations for thicker wall. However, the order is reversed after thickness correction, with the estimation for 4.5mm wall being slightly larger than that for 6mm wall. Again it is seen that thickness-corrected HSS evaluations are in good agreement with the lower bound of one-millimeter stress approach estimation, while the uncorrected is excessively conservative.

7. CONCLUSIONS

In this study, features of stress concentration and deformation of normal, ring-strengthened and U-stiffener type post structures are comprehensively studied with 3D FEM analyses. Based on the analytical results, fatigue estimations are conducted with both HSS method and one-millimeter stress approach suggested by the writers. Available fatigue test results are also presented. The main points can be concluded as follows.

In normal type post structures, high stress con-

centration exists at gusset tip region. Under axial loading, significant outward deformation occurs at gusset tip while the post wall in between neighboring gussets deforms inward. Bending loads generate comparable stress concentration at tensile gusset tip to axial loading.

Compared with analytical results of solid model, shell element model leads to increased stress concentration and high stress gradient at critical point region due to neglect of weld geometry.

Stress concentration at gusset tip increases with post wall thickness, and decreases with increase in baseplate thickness, post diameter, or gusset length. Boundary condition of baseplate has more significant effect on stress concentration at gusset tip, but favorable conditions are difficult to realize. Adopting improved forms of post structures, e.g., ring-strengthened or U-stiffener types, is more effective in reducing stress concentration and deformation at critical points.

Test results show that the fatigue strength of normal type post structure ranges from JSSC-F to H, and that fatigue strength of U-stiffener type is higher than JSSC-C. It seems appropriate to suggest the fatigue strength of JSSC-H and C for normal and U-stiffener type, respectively. Test data are not available for ring-strengthened type, and the fatigue strength of 66MPa at 2 million cycles can be estimated in terms of stress at one-millimeter in depth for bending loads, which is comparable to JSSC-F Category (65MPa at 2 million cycles).

One-millimeter stress approach gives estimations in good agreement with fatigue test results for normal type post structures. In the case of U-stiffener post structures, the estimation of one-millimeter stress approach is lower than fatigue test results.

HSS method leads to excessive underestimation for both normal and U-stiffener type post structures. The inclusion of the bonus thickness effect makes the estimation consistent with that of one-millimeter stress approach and test data, which indicates that thickness correction is necessary for estimation of post structures with HSS method.

ACKNOWLEDGMENT: The writers wish to thank Nippon Steel Corporation, NKK, Sumimoto Construction Materials of Metal, and Dept. of Civil Engineering of Aichi Institute of Technology for providing part of the test data and valuable advice, and thanks are also due to Prof. X. L. Zhao in Monash University, Australia for comments. This research is supported by the Ministry of Education, Science, Sports and Culture, Grant-in-Aid for Scientific Research (B), 50109310, 2002.

REFERENCES

1) Japan Highway Association, *Guidelines for Fatigue Design of Steel Highway Bridges*, 2002.
2) Ojio, T., Lee, S., Yamada, K., Mori, N., and Morishita, N.: Fatigue durability of sign frames due to traffic-induced vibration, *J. Struct. Engrg.*, JSCE, Vol.47(A), pp.1009-1017, 2001. (In Japanese)
3) Gilani, A. and Whittaker, A.: Fatigue-life evaluation of steel post structures. I: Analysis, *J. Struct. Engrg.*, ASCE, Vol.126, No.3, pp.322-330, 2000.
4) Gilani, A. and Whittaker, A.: Fatigue-life evaluation of steel post structures. II: Experimentation, *J. Struct. Engrg.*, ASCE, Vol.126, No.3, pp.331-340, 2000.
5) Japanese Society of Steel Construction (JSSC): *Fatige Design Recommendations for Steel Structures [English Version]*, 1995.
6) British Standards Institution (BSI): *Steel, Concrete, and Composite Bridges, Part 10, Code of Practice for Fatigue*, 1980.
7) American Association of State Highway and Transportation Officials (AASHTO): *Standard Specifications for Highway Bridges, Fifteenth Edition*, 1992.
8) Zhao, X. L., Herion, S., Packer, J. A., Puthli, R. S., Sedlacek, G., Wardenier, J., Weynand, K., van Wingerde, A. M., and Yeomans, N. F.: *Design Guide for Circular and Rectangular Hollow Section Welded Joints under Fatigue Loading*, TÜV-Verlag, Köln, Germany, 2001.
9) Hobbacher, A.: *Recommendations on Fatigue of Welded Components*, IIW document XIII-1539-95/XV-845-95, 1995.
10) Yamada, K., Xiao, Z. G., Kim, I. T., and Tateishi, K.: Re-analysis of fatigue test data of attachments based on stress at fillet weld toe, *J. of Struct. Engrg*, JSCE, Vol.48(A), pp.1047-1054, 2002. (In Japanese)
11) Structural Research and Analysis Corp. (SRAC): *COSMOS/M User's Guide*, COSMOS/M 2.6 online help documents, 2000.
12) Lazzarin P., and Tovo, R.: A notch stress intensity factor approach to the stress analysis of welds. *Fatigue and Fracture of Engineering Materials and Structures*, Vol.21, pp.1089-1103, 1998.
13) van Wingerde, A. M., Packer, J. A., and Wardenier, J.: Criteria for the fatigue assessment of hollow structural section connections, *J. Construct. Steel Research*, Vol. 35, pp.71-115, 1995.
14) Niemi, E. and Marquis, G.: Introduction to the structural stress approach to fatigue analysis of plate structures, *Proceedings of the IIW Fatigue Seminar*, IIW-commission XIII, Tokyo, 2002.
15) Yamada, K., Kondo, A., Kobayashi, K., Miyamoto, S., and Araki, J.: Fatigue strength of steel lighting pole's tubular flange joints, *J. Struct. Engrg.*, JSCE, Vol.38(A), pp.1045-1054, 1992. (In Japanese)
16) Nippon Steel Corporation, *Technical Materials of Nippon Steel Corporation*, 2000.

(Received October 21, 2002)